ACS APPLIED MATERIALS & INTERFACES

Research Article

Cite This: ACS Appl. Mater. Interfaces 2019, 11, 26433−26441

www.acsami.org

Ultrastable Water-in-Oil High Internal Phase Emulsions Featuring Interfacial and Biphasic Network Stabilization

Michelle C. Lee, Chen Tan, Raheleh Ravanfar, and Alireza Abbaspourrad*

Department of Food Science, Cornell University, Stocking Hall, Ithaca, New York 14853, United States

Supporting Information

ABSTRACT: In this work, we present gel-in-gel water-in-oil (W/O) high internal phase emulsions (HIPEs) that feature high stability by structuring both phases of the emulsion. Compared to significant advances made in oil-in-water (O/W) HIPEs, W/O HIPEs are extremely unstable and difficult to generate without introducing high concentrations of surfactants. Another main challenge is the low viscosity of both water and oil phases which promotes the instability of W/O HIPEs. Here, we demonstrate ultrastable W/O HIPEs that feature biphasic structuring, in which hydrogels are dispersed in oleogels, and self-forming, low-concentration interfacial Pickering crystals provide added stability. These W/O HIPEs exhibit high tolerance toward pH shock and destabilizing environments. In addition, this novel ultrastable gel-in-gel W/O HIPE is sustainable and made solely with natural ingredients without the addition of any synthetic stabilizers. By applying phase structuring within the HIPEs through the addition of various carrageenans and beeswax as structurants, we can increase the emulsion's stability and viscoelastic rheological properties. The performance of these gel-in-gel W/O HIPEs holds promise for a wide range of applications. As a proof of concept, we demonstrated herein the application as a gelled delivery system that enables the co-delivery of hydrophilic and hydrophobic materials at maximized loads, demonstrating high resistance to gastrointestinal pHs and a controlled-release profile.

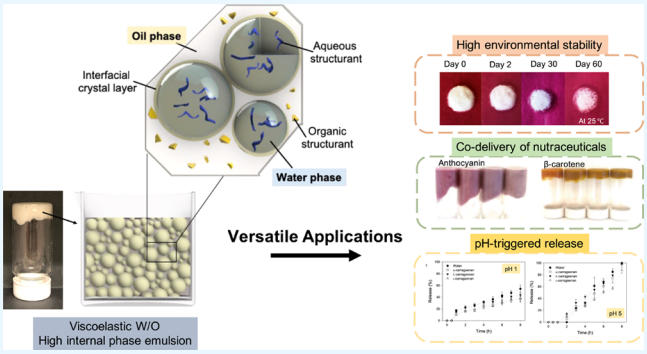

KEYWORDS: *high internal phase emulsion, W/O emulsion, gel-in-gel, phase structuring, oleogel, carrageenan*

1. INTRODUCTION

High internal phase emulsions (HIPEs) are highly concentrated gelled emulsions with an internal phase volume fraction (Φ) exceeding 0.74.[1] When the internal phase volume fraction exceeds this value, the dispersed droplets reach their maximum packing density and give rise to highly viscoelastic flow behavior. Because of these viscous flow characteristics, HIPEs have gained popularity for numerous applications, including as templates for porous materials,[2] foams,[3] and cosmetic products,[4] as solid supports for surface modification[5] and functional food,[6] and as scaffolds for tissue engineering.[7]

Despite the highly viscoelastic behavior, HIPEs are not kinetically or thermodynamically stable. Typically, the formation of stable HIPEs requires the addition of low molecular weight surfactants[8] or alternatively the addition of solid colloidal particles in the continuous phase to form Pickering HIPEs.[9] The selection of surfactants is also critical to form stable HIPEs and often requires large quantities.[10] Although Pickering HIPEs have shown increased stability compared with surfactant-stabilized HIPEs, their formation requires chemically tailored particles with appropriate hydrophobicity, and the resulting emulsion still remains susceptible to phase inversion at high Φ.[11,12]

Water-in-oil (W/O) HIPEs are more difficult to fabricate because of the lack of hydrophobic natural stabilizers, resulting in the limited exploration of these materials.[13−15] In addition, the high surface tension of water can also lead to immediate phase inversion during HIPE fabrication when the internal phase volume fraction is high.[16] Moreover, conventional W/O HIPEs are often stabilized with synthetic surfactants, which can negatively affect the environment and human health.[17] Despite the fact that some more environmentally friendly W/O HIPEs have been developed, they require complicated and time-consuming modification of the stabilizers (e.g., starch or polysaccharide).[14,15] Therefore, facile methods to form stable and sustainable W/O HIPEs are still in high demand.

In this study, we propose a simple strategy of generating W/O HIPEs upon temperature stimulation to induce the spontaneous formation of Pickering crystals and biphasic networks. We utilize biodegradable surfactant glycerol monooleate (GMO), a glycerol fatty ester that can solidify and form fat crystals, to provide spontaneous interfacial Pickering stabilization of the W/O emulsion.[18,19] Additionally,

Received: March 21, 2019
Accepted: June 27, 2019
Published: June 27, 2019

DOI: 10.1021/acsami.9b05089
ACS Appl. Mater. Interfaces 2019, 11, 26433−26441

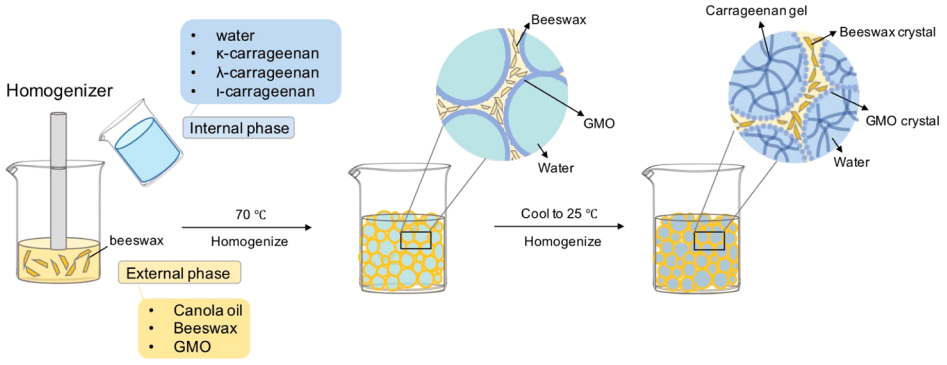

Figure 1. Schematic illustration of the fabrication of W/O HIPEs with different phase structuring.

we have added structurants in both phases, generating carrageenan hydrogel in the internal aqueous phase and beeswax-containing oleogel in the external oil phase. When the network is increased in both phases, or biphasically, we enable the formation of ultrastable gel-in-gel HIPEs with volume fractions as high as 0.80. By tuning the network of each phase, the resultant gel-in-gel HIPEs demonstrate improved stability, avoid phase inversion during fabrication, and can be used as a potential drug co-delivery system. We systematically investigate the role of this interfacial and biphasic structuring on HIPE stability, with the demonstration of protection and release of bioactive compounds for potential application in nutraceutical and biomedical-related fields.

2. MATERIAL AND METHODS

2.1. Materials. Fluorescein isothiocyanate (FITC) isomers (≥90.0%), Nile red, β-carotene (type I, synthetic, >93% purity), and sodium hydroxide (≥98.0%) were purchased from Sigma-Aldrich (St. Louis, MO, USA). Hydrochloric acid (36.5−38%) was obtained from VWR International (Radnor, PA, USA). Canola oil was purchased from a local supermarket (Ithaca, NY, USA). Kappa (κ), iota (ι), and lambda (λ)-carrageenan was provided by TIC Gums Incorporated (White Marsh, MD, USA). GMO (Capmul GMO-50 EP/NF) was kindly donated by Abitec Corporation (Columbus, OH, USA). Beeswax was kindly donated by Strahl & Pitsch, Inc. (West Babylon, NY, USA). The anthocyanin used was obtained from blueberry extract from Bulk Supplements (Henderson, NV, USA). All other chemicals used were of analytical grade.

2.2. Preparation of HIPEs. In brief, the oil phase consisted of 1 wt % GMO in canola oil and was heated to 70 °C. Distilled water at 70 °C was added slowly to the heated oil mixture with constant high-shear homogenization at 10 000 rpm (T25 digital ULTRA-TURRAX, IKA Works, Wilmington, NC, USA). With continuous homogenization, the HIPEs were submerged in an ice bath to cool down to 25 °C. The internal phase volume fraction was calculated as the volume of the water phase included in the emulsion divided by the total volume of the emulsion. For oleogel-HIPEs (O-HIPE), beeswax (0.5, 1, 3, 5, and 10 wt %) was additionally melted into the oil phase to increase the structure of the external phase. For gel-in-gel HIPEs, additional 1 wt % carrageenans (κ-/ι-/λ-) were incorporated in the water phase of the O-HIPE to increase the structure of the internal phase.

2.3. Rheological Measurements of HIPEs. The O-HIPEs and gel-in-gel HIPEs were stored and measured at 25 °C. Dynamic rheological measurements were conducted on an AR 1000 rheometer (TA Instruments, New Castle, DE, USA) using a 40 mm plate geometry and a gap of 500 μm. The linear viscoelastic region was determined by a strain sweep at a frequency of 1 Hz from 0.0001 to 10. The G' and G'' modulus was obtained through frequency sweeps from 0.1 to 10 rad/s using a fixed strain value of 0.0003.

2.4. Microscopy. The microstructures of the HIPEs were inspected with a confocal laser scanning microscope (LSM 710, Carl Zeiss, Göttingen, Germany) and a cryo-scanning electron microscope [FEI Strata 400S Dual Beam focused ion beam/scanning electron microscopy (FIB/SEM) system]. For confocal laser scanning microscopy (CLSM), the internal and external phases were stained with FITC and Nile red at 1 and 2 mg/mL, respectively. The HIPE structural morphology was studied using excitation/emission wavelengths of 488/515 and 492/518 nm for FITC and Nile red, respectively. For cryo-SEM imaging, the HIPEs were prepared by plunge-freezing into slush nitrogen and transferred under vacuum into the system (Quorum PP3010T cryo-FIB/SEM preparation system, Quorum Technologies, Newhaven, UK). The sample was then maintained at −165 °C, cross-sectioned with a fracturing knife, and coated with gold−palladium. Images were collected at 3 kV, with a working distance of 5 mm. Energy-dispersive X-ray spectroscopy (EDS) was performed during cryo-SEM imaging for spot element analysis. EDS was carried out using an accelerating voltage of 10 kV, and the data were collected and analyzed through INCA software (Oxford Instruments, Concord, MA, USA).

2.5. Measurement of Contact Angle. Contact angles of the internal phase on glass surfaces coated with 1% GMO and different concentrations of beeswax (0.5−10%) used in the external phase mixtures were measured using a tensiometer (ramé-hart model 500, Succasunna, NJ, USA). Approximately 5 μL of the internal phase was dispensed on the surface, and contact angles were analyzed through DROPimage Advanced software (ramé-hart co., Succasunna, NJ, USA).

2.6. Particle Size Measurement. To measure the mean particle diameters of the droplets within the HIPE samples, we utilized ImageJ software (v1.51, National Institute of Health, USA) for image analysis. This software calculates the droplet diameter through image pixel analysis. At least 100 particles were analyzed for each sample.

2.7. Physical Stability of HIPEs. HIPEs were formed into a round disk-shape 1.5 cm in diameter and with a thickness of 0.5 cm. Images of these HIPE disks were taken after being dried for 2, 30, and 60 days under open air at 25 °C.

2.8. Anthocyanin and β-Carotene in Vivo Release. To demonstrate the use of the resulting HIPEs as a potential nutraceutical/drug delivery system, we prepared anthocyanin-loaded HIPEs and anthocyanin/β-carotene co-loaded HIPEs to monitor the release of the anthocyanin and β-carotene under pH values of 1 and 5. Briefly, 1.25 mg/mL of the anthocyanin was incorporated into the internal phase at pH 5, and 1 mg/mL of the β-carotene was incorporated into the external phase. The anthocyanin-loaded HIPEs and anthocyanin/β-carotene co-loaded HIPEs were prepared using the same methods for HIPE fabrication described previously. The in vitro release of the anthocyanin and β-carotene were based on the membrane-free model with slight modifications.[20] Approximately 100 mg of the HIPEs was weighed into glass vials, followed by the careful addition of water adjusted to pH 1 or 5. Simultaneously, canola oil was added into the vials, at which point the HIPEs reside between the water and oil interface. The glass vials were then shaken within a

DOI: 10.1021/acsami.9b05089
ACS Appl. Mater. Interfaces 2019, 11, 26433−26441

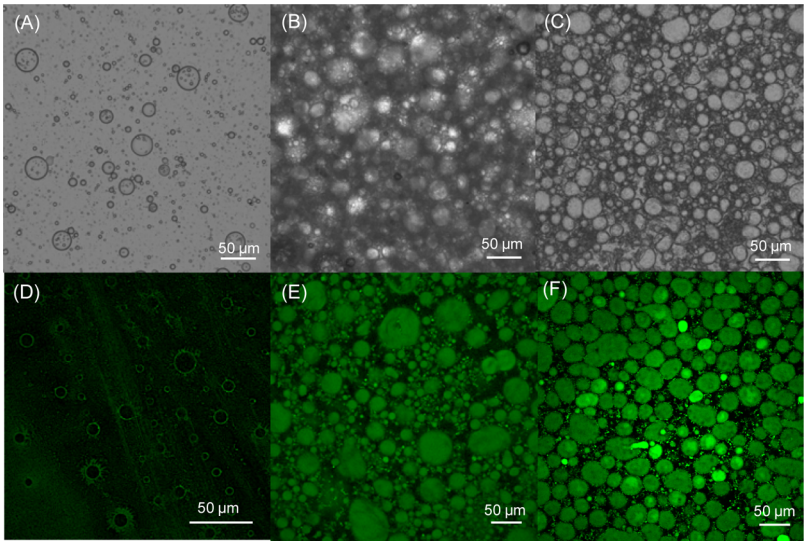

Figure 2. (A–C) Optical and (D–F) CLSM images of the HIPE microstructures stabilized by (A,D) 1 wt % GMO, (B,E) 3 wt % beeswax, and (C,F) both 1 wt % GMO and 3 wt % beeswax in the external phase at Φ = 0.75. FITC is incorporated as the only water-soluble indicator.

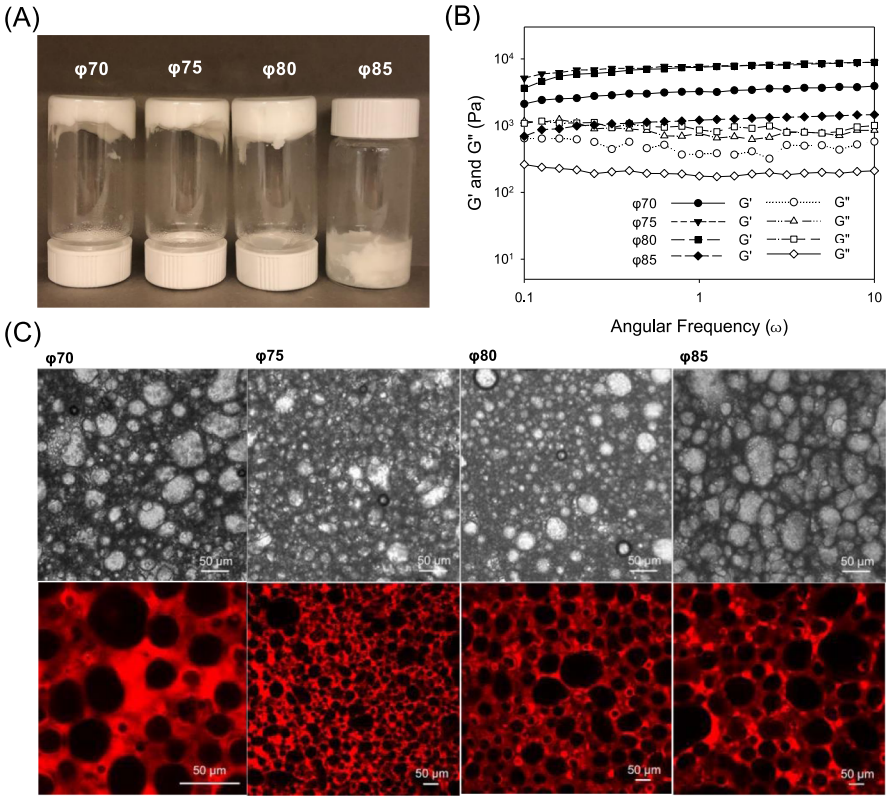

Figure 3. O-HIPEs featuring different internal phase volume fractions. (A) Images and (B) rheological measurements of O-HIPEs prepared at different internal phase volume fractions. (C) Microstructure of different internal phase volume fraction O-HIPEs as shown by (top) optical microscopy and (bottom) CLSM.

water bath at 37 °C. At specific time intervals, aliquots of fluid from the water and oil phases were withdrawn and replaced by the same volumes of fresh water and oil medium. The amount of the released anthocyanin and β-carotene were measured using ultraviolet–visible (UV–vis) spectrophotometry (UV-2600, Shimadzu Scientific Instrument, Marlborough, MA, USA) at 520 and 452 nm, respectively.[21,22] The released amounts were calculated as the anthocyanin/β-carotene in the collected medium at a given time divided by the initial anthocyanin/β-carotene in the HIPEs and multiplied by 100. Each experiment was performed in triplicate, and the results were reported as mean ± standard deviation.

3. RESULTS AND DISCUSSION

3.1. Oleogel-HIPEs. Figure 1 shows the HIPE preparation process. Successful HIPE formation is dependent on the ability to incorporate more than 74 vol % of internal phase into the external phase. However, phase inversion occurs easily for W/O HIPEs because of the high interfacial surface tension and the

DOI: 10.1021/acsami.9b05089
ACS Appl. Mater. Interfaces 2019, 11, 26433–26441

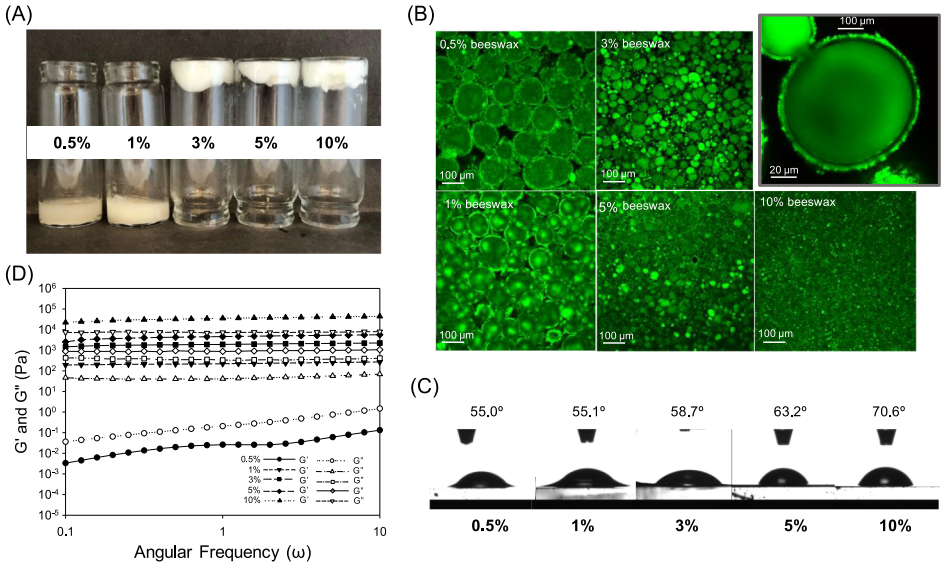

Figure 4. Fabrication of O-HIPEs at Φ = 0.75 using different beeswax concentrations in the external phase. (A) Image of the O-HIPEs formed at different wax concentrations in the external phase. (B) Microstructure of the O-HIPEs shown via CLSM imaging. FITC is incorporated as the only water-soluble indicator. (C) Contact angle measurements of water on oleogel films of 1 wt % GMO and different beeswax concentrations (0.5−10 wt %). (D) Rheological measurements of the O-HIPEs structured with different wax concentrations.

low viscosity of the internal phase.[1] To overcome these limitations and form stable HIPEs, surfactants that are insoluble in the internal phase are typically required to lower the interfacial surface tension. We therefore used 1 wt % GMO, a natural biodegradable amphiphilic lipid as a surfactant to stabilize the W/O emulsions to form HIPEs by interfacial stabilization. However, lowering the interfacial surface tension alone does not promote W/O HIPE formation at Φ = 0.75 (Figures 2A,D and S1A). Instead, phase inversion occurred, thus becoming an oil-in-water (O/W) emulsion, possibly because of low GMO surface activity, which is insufficient to stabilize high internal fractions. Previous research has reported similar outcomes when GMO is applied at higher concentrations of 5 wt %.[23] Alternatively, we explored the use of a network stabilization method, which involves increasing the structure and viscosity of the external phase to stabilize the internal phase. Therefore, we added 3 wt % beeswax to the external phase as a structurant to form an oleogel thin film between the internal phase droplets (Figure 2B,E). However, HIPEs made solely with beeswax have low stability, in which the dispersed phase showed a large average droplet diameter (28.86 ± 11.33 μm) and phase-separated over a day (Figure S1B, Table S1). As a comparison, the HIPE formed by adding both the surfactant (GMO) and structurant (beeswax) to the external phase increased the HIPE stability, as demonstrated by the smaller (17.59 ± 6.18 μm) and more uniform size of the resulting droplets (Figures 2C,F, S1C, Table S1). Therefore, a combination of GMO at low concentration and beeswax in the external phase endows the HIPE with both interfacial and network stabilization, a material we refer to as an O-HIPE, which features a single oleogel structured external phase.

Next, we investigated the effect of different internal volume fractions (Φ) of water using fixed 1 wt % GMO and 3 wt % beeswax as stabilizers. As demonstrated in Figure 3A, the highly concentrated emulsion can form gels with internal volume fractions of up to 0.80. Additionally, rheological measurements show that O-HIPEs with internal fractions of 0.75 and 0.80 demonstrate the highest storage modulus (G') value, indicating stronger viscoelasticity behavior (Figure 3B). However, at Φ = 0.80, the droplet sizes are not the smallest (40.42 ± 14.77) among all the samples prepared, but are the most tightly packed (Figure 3C, Table S2). Interestingly, a viscoelastic O-HIPE was formed at Φ = 0.70, even though the volume did not reach the packing density of Φ = 0.74.[1] This was possibly due to the oleogel structure that increased the external phase viscosity, which lowered the packing density but still enabled a gel-like structure.[1,24] Considering the microstructure of O-HIPEs with different internal fractions, the average particle sizes of the internal phase are smaller and more uniform at Φ = 0.70 (27.16 μm) and Φ = 0.75 (25.78 μm), with larger particle sizes and wider particle size distribution at Φ = 0.80 (40.42 μm) and Φ = 0.85 (45.77 μm) (Figure S2, Table S2). Typically, a larger particle size would indicate the instability of the HIPEs overtime, as smaller particle sizes feature increased surface area and thus higher packing density and stability.[22] The instability that arises from larger droplet particle sizes was further shown in a storage study, in which we observed that macroscopic separation occurred in O-HIPEs of Φ = 0.80 and Φ = 0.85 over 2 days of storage (Figure S3). Therefore, we selected a volume ratio of Φ = 0.75 for all subsequent emulsions studied.

Mechanically, a more viscous and rigid external phase can increase the O-HIPE stability but will result in a lower maximum internal phase volume.[1,24,25] Therefore, we studied the effect of beeswax concentration on the rheological behavior and overall ability to form O-HIPEs. Figure 4A shows that at Φ = 0.75, a beeswax concentration of greater than 3 wt % is necessary for the formation of the O-HIPE. The microstructure of the O-HIPE also varied with beeswax concentration (Figure 4B). Strikingly, the high magnification image of a single aqueous droplet under CLSM showed a distinct interfacial layer formed with surface-active particles, suggesting that our O-HIPEs are potentially Pickering HIPEs (Figure 4B, inset). This observation is similar to a previous study, demonstrating that at high temperature, GMO dissolves in the oil external phase and then forms GMO crystals around the

DOI: 10.1021/acsami.9b05089
ACS Appl. Mater. Interfaces 2019, 11, 26433−26441

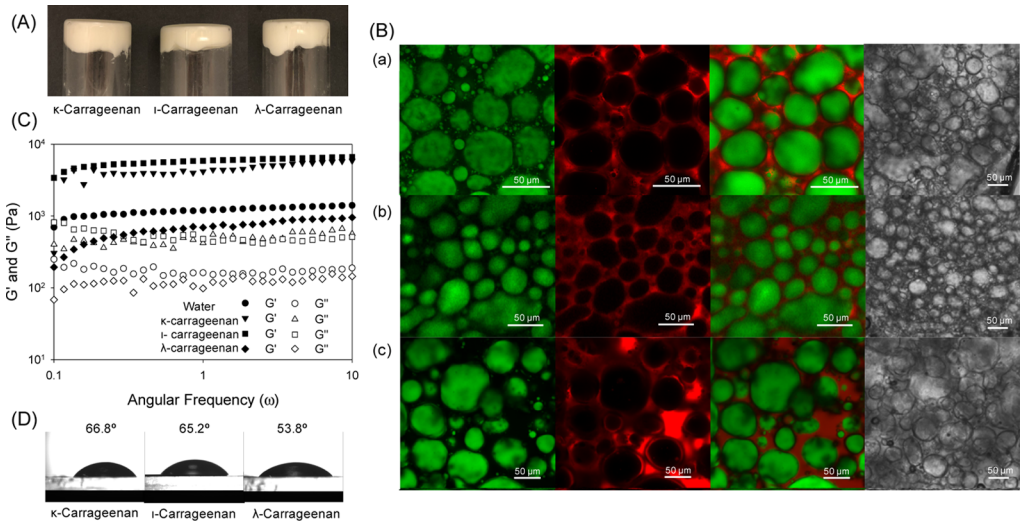

Figure 5. Fabrication of HIPEs at Φ = 0.75 with 3 wt % beeswax and 1 wt % GMO and different types of carrageenans in the internal phase at 1 wt %. (A) Images of the gel-in-gel HIPEs. (B) Microstructure of these HIPEs made with (a) κ-carrageenan, (b) ι-carrageenan, and (c) λ-carrageenan in the internal phase, as shown by CLSM (in the left three columns, the aqueous and oil stains are represented by the green and red colors, respectively) and optical microscopy (right column). (C) Rheological measurements of the HIPEs that were internally structured with different types of carrageenans. (D) Contact angle measurements of the different types of carrageenan on the oleogel film consisting of 3 wt % beeswax and 1 wt % GMO.

aqueous droplets when cooled.[26] Interestingly, these GMO crystals can originate from the external phase as pre-formed crystals and/or act as a surfactant, which solidifies at the droplet interface.[18,27] Additionally, previous research had demonstrated molten wax's role in W/O emulsions, in which rapidly cooling waxes contribute to the increased structure of the external phase, thus providing network stabilization.[28] This was evident in interfacial tension measurements, where GMO addition lowers the internal phase surface tension but beeswax addition does not (Figures S4 and S5). Therefore, with a fixed GMO concentration of 1 wt %, Figure 4 demonstrates beeswax's main role in external network building. The effect of beeswax concentration on the network stabilization can be demonstrated by measurement of contact angle (Figure 4C) and bulk oleogel properties (Figure S6). We measured the contact angle by dispensing water on different oleogel films made with 1 wt % GMO and beeswax concentrations of 0.5−10 wt % (Figure 4C). We observed the lowest contact angle at 0.5−1 wt % beeswax (55.0°), which slightly increased at 3 wt % (58.7°), followed by a steady increase at 5 wt % (63.2°) and 10 wt % (70.6°). Water wetted the oleogel film to a more noticeable degree at 0.5−1% beeswax, demonstrating the flowability of both phases and the low external network. For bulk oleogel, we incorporated beeswax in the oil to increase the network (Figure S6). We determined a cutoff point of 3 wt % beeswax was necessary to form a self-standing bulk oleogel (Figure S6A) and observed increased storage moduli (G') at higher beeswax concentration (Figure S6B), which is consistent with the rheological trend of the O-HIPEs (Figure 4D). Together, it is evident that the O-HIPEs are dependent on the strength of the external network. With low external network, such as 0.5−1 wt % beeswax, O-HIPEs cannot be formed. However, for high external networks, such as 10 wt % beeswax, the O-HIPEs are not sufficiently stable.

We also found that the beeswax concentration affected the particle size and size distribution (Figure S7, Table S3); 0.5 and 1 wt % beeswax in the external phase showed multimodal particle distributions and large particle sizes, suggesting the inability to form O-HIPEs. When studying the rheological behavior of the O-HIPEs, we observed that G' increases with increasing beeswax concentration (Figure 4D). Because of the lack of external structure, 0.5 wt % beeswax resulted in the lowest G', and in which $G'' > G'$, indicating more liquid-like behavior.[29] Although the O-HIPE with 10 wt % beeswax showed the highest G', suggesting the best stability, it was not stable as phase separation occurred when stored over 2 days (Figure S8). This is due to the extensive external network provided by the 10 wt % beeswax upon cooling, the high viscosity of which prevents efficient homogenization during fabrication, thus lowering the amount of internal phase that can be incorporated.[1,24] Therefore, we believe that the highest viscoelastic behavior for O-HIPEs with 10 wt % beeswax is a result of the excess bulk beeswax network in the external phase. In addition, O-HIPEs formed with 5 wt % beeswax did not show a higher rheological performance as compared with samples made with 3 wt % beeswax. This cutoff threshold indicates an optimal beeswax concentration of 3 wt % (Figure 4D). Overall, we have demonstrated formation of O-HIPEs by combining Pickering GMO and a beeswax network for high internal aqueous phase stabilization.

3.2. Gel-in-Gel HIPEs. In addition to structuring the external phase, we further increased the network of the internal phase using carrageenans, which are polysaccharides typically used as thickening and gelling agents.[30] We refer to such HIPEs, with both phases structured, as gel-in-gel HIPEs. Building upon the most stable O-HIPE containing 3 wt % beeswax, the internally structured HIPEs can be successfully formed with various types of carrageenan, including κ-, ι-, and λ-carrageenan (Figure 5A) at 1 wt % (Figure S9). Microscopy imaging reveals that the gel-in-gel HIPEs formed with ι-carrageenan feature the smallest droplet sizes (27.18 ± 12.95 μm) and the highest packing morphologies, while those formed with κ-carrageenan and λ-carrageenan showed similar packing microstructures, but with larger particle sizes (Figure 5B, Table S4).

DOI: 10.1021/acsami.9b05089
ACS Appl. Mater. Interfaces 2019, 11, 26433−26441

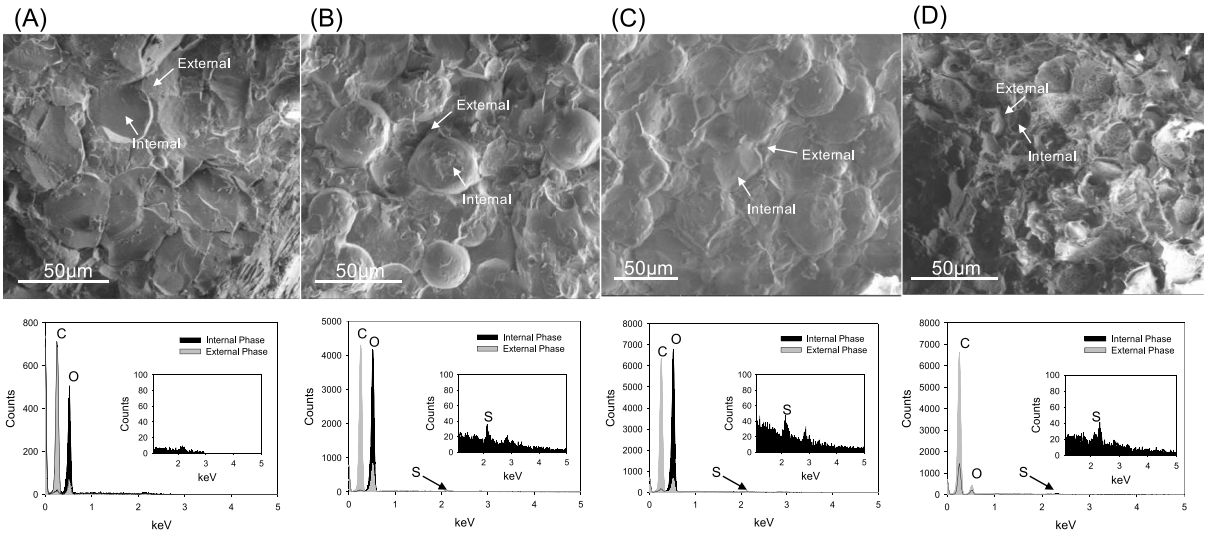

Figure 6. Cryo-SEM (top row) images and EDS (bottom row) measurements of the (A) O-HIPE and (B–D) gel-in-gel HIPEs made with (B) κ-carrageenan, (C) ι-carrageenan, and (D) λ-carrageenan.

In terms of the rheological performance (Figure 5C), ι-carrageenan endowed the gel-in-gel HIPE with the strongest viscoelasticity, followed by κ-carrageenan. By increasing the network in the internal phase, gel-in-gel HIPEs can increase the viscoelastic behavior by more than 5-fold compared to the corresponding O-HIPE, except for λ-carrageenan, which features a G' value even lower than the O-HIPE. This may be explained by the fact that λ-carrageenan is the most sulfated carrageenan and has a flat structure, which makes it a non-gelling thickening agent.[30] In addition, the shear-thinning characteristics of λ-carrageenan enable it to be incorporated into the gel-in-gel HIPE's internal phase, but it is incapable of maintaining the rigid structure over time and wider ranges of the particle size distribution are observed (Figure S10). Interestingly, the contact angles of pure κ- and ι-carrageenan are higher, while that of λ-carrageenan is lower than that of water on a 3 wt % beeswax oleogel film (Figures 4C and 5D). The lower contact angle measurement suggests that λ-carrageenan has more affinity toward the external phase, leading to the instability of the dispersed aqueous phase.

We attribute the formation of these gel-in-gel HIPEs to the increased structuring in both phases. To better understand the HIPE structure and the materials at each phase, we performed cryo-SEM imaging and EDS elemental analysis, respectively. Figure 6 shows the packing of the O-HIPE and gel-in-gel HIPE droplets with defined borders between the internal and external phases and a clear visualization of the droplet structure. The gel-in-gel HIPEs formed with λ-carrageenans showed less distinct droplet morphologies, which would result in less packing and thus lower stability, which is consistent with the sample's rheological behavior (Figure 5C). We also performed EDS analysis on the apparent internal and external phase regions. Theoretically, in W/O HIPEs, the internal phase should be composed of a higher oxygen content because of the greater presence of water compared to the external phase, which should be composed mostly of carbon from canola oil and beeswax. Table S5 displays approximate atomic percentages of each detected element from the EDS analysis. We found that the internal phase was mostly composed of oxygen, whereas the external phase consisted of mostly carbon. Although both the internal and external phases of the λ-carrageenan sample showed higher carbon content compared to oxygen, a significant sulfur peak appeared in the analysis of the internal phase (Figure 6D, inset). This sulfur peak is from λ-carrageenan, which contains 3 sulfur groups per 2 sugar molecules in its chemical structure. Here, we confirmed that carrageenans are trapped within the internal phase, which greatly assist in internal network stabilization.

3.3. Stability Assessment. It is essential to investigate the stability of emulsions during a given storage period, as emulsions are thermodynamically unstable with a tendency to coalesce. Figure 7 demonstrates the stability of the O-HIPE and gel-in-gel HIPEs over 2 months at 25 °C in open atmosphere. We observed that the O-HIPE remained stable up to day 2 but collapsed after 30 days with a transparent appearance. In contrast, the gel-in-gel HIPEs maintained their structure, remaining opaque over 2 months, indicating the presence of an emulsion structure.[31] We attribute the differences in stability to the interfacial and network stabilization of the gel-in-gel HIPEs, in which the internal aqueous droplets with high viscosity are less prone to coalescence and are protected by an external layer of solid oil, which prevents evaporation. Results from accelerated

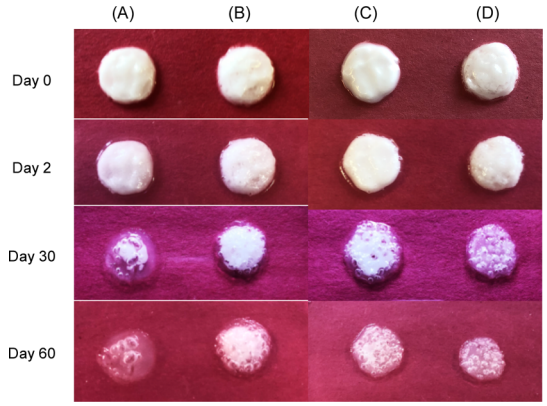

Figure 7. Images of the (A) O-HIPE and gel-in-gel HIPEs made from (B) κ-carrageenan, (C) λ-carrageenan, and (D) ι-carrageenan stored over time at 25 °C in open atmosphere.

DOI: 10.1021/acsami.9b05089
ACS Appl. Mater. Interfaces 2019, 11, 26433–26441

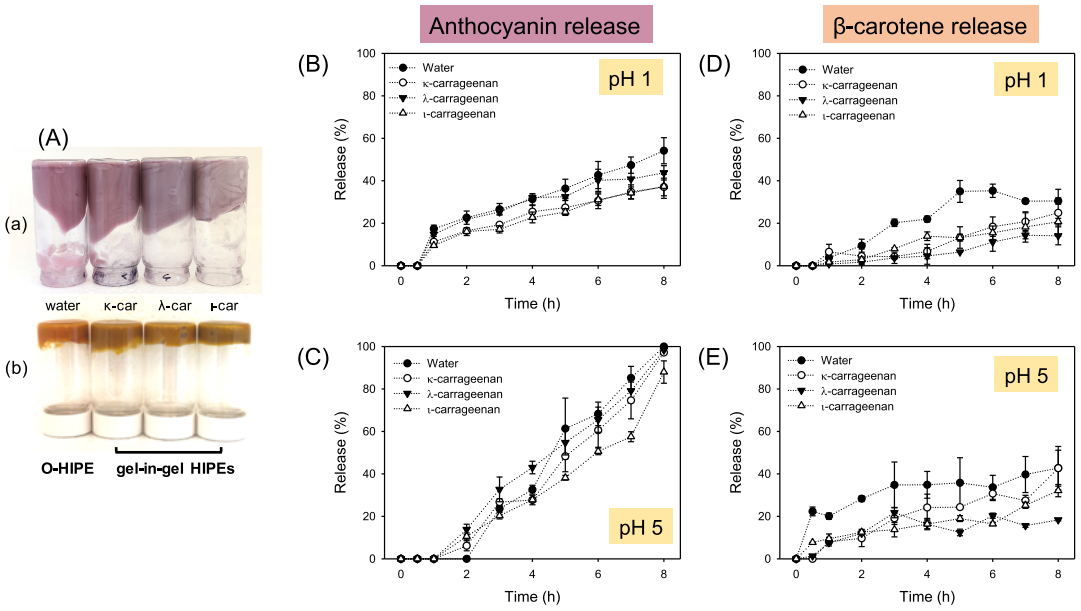

Figure 8. Incorporation of anthocyanin and β-carotene into O-HIPE and gel-in-gel HIPEs. (A) Images showing (a) anthocyanin-incorporated and (b) anthocyanin/β-carotene incorporated O-HIPE and gel-in-gel HIPEs. The release of anthocyanin at 37 °C from O-HIPE and gel-in-gel HIPEs at (B) pH 1 and (C) pH 5, and the release of β-carotene at (D) pH 1 and (E) pH 5.

storage studies under vacuum (Figure S11) and 37 °C (Figure S12) are concordant. This excellent stability of the gel-in-gel HIPEs is due to the tightly packed internal phase that is internally stabilized by carrageenans, interfacially stabilized by the GMO, and externally stabilized by the beeswax network.

3.4. In Vitro Release of Anthocyanin and β-Carotene.

Our strategy for forming ultrastable HIPEs involves a structured biphasic system of both oil and aqueous phases, and unlike conventional W/O emulsions consisting of a liquid-in-liquid model with more flowability, this unique gel-in-gel HIPE enables loading of both hydrophilic and hydrophobic nutraceuticals immobilized in the internal and external phases, respectively. To understand the responsiveness of the gel-in-gel HIPEs under pH shock, we utilized anthocyanin as a model hydrophilic bioactive because of its health benefits and its high sensitivity to pH. At acidic pH, anthocyanins are red and gradually shift to a purple to blue color as the pH value increases[32,33] We hypothesized that with the help of biphasic structuring in our gel-in-gel HIPE, the entrapped anthocyanin would be greatly protected against environmental changes. Figure 8Aa shows the anthocyanin-incorporated O-HIPE and gel-in-gel HIPEs. At 25 °C, the anthocyanin-containing HIPEs showed no color change over 7 days of storage in solutions of different pHs (1−8) (Figure S13A). This outstanding color stability is comparable to other color stabilization methods, such as layer-by-layer encapsulation[34] and copigmentations,[35] as anthocyanin is highly unstable at pH 8. At a higher temperature (37 °C) simulating the human body, anthocyanin releases slowly, as such a temperature approaches the melting temperature of internal carrageenans (40 °C). Despite partial disintegration of carrageenans, up to 45−70% of the original anthocyanin remained after 8 h at pH 1 (Figure 8B). We also observed that gel-in-gel HIPEs made with κ-carrageenan and ι-carrageenan retained anthocyanin the best, while λ-carrageenan retained anthocyanin similarly to the O-HIPE. At pH 5, the release of anthocyanin was faster (Figure 8C), which is likely because at pH 5 anthocyanin will be deprotonated in the internal phase. This deprotonation induces GMO's crystal structural change at the HIPE droplet interfaces and stabilizes as a bicontinuous cubic phase because of the electrostatic repulsion between negatively charged anthocyanin and the negatively charged headgroups of GMO.[36] Such changes of the GMO crystal structure allow higher water absorptivity and thus a higher release rate.[36,37]

In addition to hydrophilic compounds, hydrophobic ones, such as β-carotene, can also be incorporated into the oleogel-structured external phase (Figures 8Ab, S13B). As shown in Figure 8D,E, β-carotene was released from the O-HIPE at a significantly higher rate ($P < 0.05$) than the gel-in-gel HIPEs. The higher release might be due to the looser packing of the O-HIPE's internal phase, and thus the β-carotene in the external phase is more prone to diffuse out. However, β-carotene incorporated in the external phase of gel-in-gel HIPEs releases in a similarly slow fashion to those that are encapsulated in the O/W Pickering HIPE.[38] These observations suggest the potential for such gel-in-gel HIPEs to be used as a long-term delivery system for both hydrophilic and hydrophobic compounds.

4. CONCLUSIONS

The combination of GMO interfacial droplet stabilization and the structured network provided by beeswax externally and carrageenan internally enables the fabrication of W/O HIPEs with excellent stability. The fabrication process utilizes renewable materials and provides a robust technique for overcoming the difficulties in forming ultrastable W/O HIPEs. These gel-in-gel HIPEs can provide insight into promising applications, such as pH-responsive release for hydrophilic and hydrophobic nutraceuticals, with high environmental stability. By creating an emulsion with biphasic structures, we enhanced the rheological behavior of current conventional W/O HIPEs. In addition, this method requires very low amounts of surfactants (0.25 wt %) and structurants (0.75 wt %) in the total system and provides high drug loading capacity. Compared to conventional polyHIPEs and Pickering HIPEs, our method exhibits great potential in terms of efficiency,

DOI: 10.1021/acsami.9b05089
ACS Appl. Mater. Interfaces 2019, 11, 26433−26441

rheological performance, encapsulation capacity, and stability. These novel gel-in-gel HIPEs, fabricated with solely natural materials, may prove valuable for the biological, chemical, food, and pharmaceutical industries.

■ ASSOCIATED CONTENT

Supporting Information

The Supporting Information is available free of charge on the ACS Publications website at DOI: 10.1021/acsami.9b05089.

Stability assays; particle size; particle size distribution; interfacial tension studies; storage and loss moduli of bulk oleogel and HIPEs; optimization of surfactants and structurants; three phase contact angle measurements; and EDS analysis (PDF)

Rheology measurements and release profile (XLSX)

■ AUTHOR INFORMATION

Corresponding Author

*E-mail: alireza@cornell.edu. Phone/Fax: +1 607 255-2923.

ORCID

Michelle C. Lee: 0000-0002-2584-7772

Chen Tan: 0000-0002-2428-9449

Alireza Abbaspourrad: 0000-0001-5617-9220

Notes

The authors declare no competing financial interest.

■ ACKNOWLEDGMENTS

This work made use of the electron microscopy and soft matter/polymer analysis facilities of the Cornell Center for Materials Research (CCMR) with support from the National Science Foundation Materials Research Science and Engineering Centers (MRSEC) program [DMR 1719875]. This work is supported by New York State Dairy Promotion Board (ESDC 88975) and the National Institute of Food and Agriculture, USDA, Hatch under 1010696.

■ REFERENCES

(1) Cameron, N. R.; Sherrington, D. C. High Internal Phase Emulsions (HIPEs)—Structure, Properties and Use in Polymer Preparation. *Biopolymers Liquid Crystalline Polymers Phase Emulsion*; Advances in Polymer Science; Springer: Berlin, 1996; Vol. *126*, pp 163–214.

(2) Hori, K.; Sano, M.; Suzuki, M.; Hanabusa, K. Preparation of Porous Polymer Materials Using Water-in-Oil Gel Emulsions as Templates. *Polym. Int.* **2018**, *67*, 909–916.

(3) Hua, Y.; Zhang, S.; Zhu, Y.; Chu, Y.; Chen, J. Hydrophilic Polymer Foams with Well-Defined Open-Cell Structure Prepared from Pickering High Internal Phase Emulsions. *J. Polym. Sci., Part A: Polym. Chem.* **2013**, *51*, 2181–2187.

(4) Magdassi, S. Delivery Systems in Cosmetics. *Colloids Surf., A* **1997**, *123–124*, 671–679.

(5) Zhao, C.; Danish, E.; Cameron, N. R.; Kataky, R. Emulsion-Templated Porous Materials (PolyHIPEs) for Selective Ion and Molecular Recognition and Transport: Applications in Electrochemical Sensing. *J. Mater. Chem.* **2007**, *17*, 2446–2453.

(6) Patel, A. R.; Rodriguez, Y.; Lesaffer, A.; Dewettinck, K. High Internal Phase Emulsion Gels (HIPE-Gels) Prepared Using Food-Grade Components. *RSC Adv.* **2014**, *4*, 18136–18140.

(7) Bokhari, M.; Carnachan, R. J.; Przyborski, S. A.; Cameron, N. R. Emulsion-Templated Porous Polymers as Scaffolds for Three Dimensional Cell Culture: Effect of Synthesis Parameters on Scaffold Formation and Homogeneity. *J. Mater. Chem.* **2007**, *17*, 4088–4094.

(8) Williams, J. M. High Internal Phase Water-in-Oil Emulsions: Influence of Surfactants and Cosurfactants on Emulsion Stability and Foam Quality. *Langmuir* **1991**, *7*, 1370–1377.

(9) Li, Z.; Ming, T.; Wang, J.; Ngai, T. High Internal Phase Emulsions Stabilized Solely by Microgel Particles. *Angew. Chem., Int. Ed.* **2009**, *48*, 8490–8493.

(10) Sun, G.; Li, Z.; Ngai, T. Inversion of Particle-Stabilized Emulsions to Form High-Internal-Phase Emulsions. *Angew. Chem., Int. Ed.* **2010**, *49*, 2163–2166.

(11) Aveyard, R.; Binks, B. P.; Clint, J. H. Emulsions Stabilised Solely by Colloidal Particles. *Adv. Colloid Interface Sci.* **2003**, *100–102*, 503–546.

(12) Kralchevsky, P. A.; Ivanov, I. B.; Ananthapadmanabhan, K. P.; Lips, A. On the Thermodynamics of Particle-Stabilized Emulsions: Curvature Effects and Catastrophic Phase Inversion. *Langmuir* **2005**, *21*, 50–63.

(13) Pang, B.; Liu, H.; Liu, P.; Peng, X.; Zhang, K. Water-in-oil Pickering emulsions stabilized by stearoylated microcrystalline cellulose. *J. Colloid Interface Sci.* **2018**, *513*, 629–637.

(14) Yang, T.; Zheng, J.; Zheng, B.-S.; Liu, F.; Wang, S.; Tang, C.-H. High Internal Phase Emulsions Stabilized by Starch Nanocrystals. *Food Hydrocolloids* **2018**, *82*, 230–238.

(15) Liu, F.; Zheng, J.; Huang, C.-H.; Tang, C.-H.; Ou, S.-Y. Pickering High Internal Phase Emulsions Stabilized by Protein-Covered Cellulose Nanocrystals. *Food Hydrocolloids* **2018**, *82*, 96–105.

(16) Welch, C. F.; Rose, G. D.; Malotky, D.; Eckersley, S. T. Rheology of High Internal Phase Emulsions. *Langmuir* **2006**, *22*, 1544–1550.

(17) Rebello, S.; Asok, A. K.; Mundayoor, S.; Jisha, M. S. Surfactants: Toxicity, Remediation and Green Surfactants. *Environ. Chem. Lett.* **2014**, *12*, 275–287.

(18) Ghosh, S.; Rousseau, D. Fat crystals and water-in-oil emulsion stability. *Curr. Opin. Colloid Interface Sci.* **2011**, *16*, 421–431.

(19) Milak, S.; Zimmer, A. Glycerol Monooleate Liquid Crystalline Phases Used in Drug Delivery Systems. *Int. J. Pharm.* **2015**, *478*, 569–587.

(20) Tan, H.; Sun, G.; Lin, W.; Mu, C.; Ngai, T. Gelatin Particle-Stabilized High Internal Phase Emulsions as Nutraceutical Containers. *ACS Appl. Mater. Interfaces* **2014**, *6*, 13977–13984.

(21) Tan, C.; Celli, G. B.; Lee, M.; Licker, J.; Abbaspourrad, A. Polyelectrolyte Complex Inclusive Biohybrid Microgels for Tailoring Delivery of Copigmented Anthocyanins. *Biomacromolecules* **2018**, *19*, 1517–1527.

(22) Tan, C.; Lee, M. C.; Pajoumshariati, S.; Abbaspourrad, A. Sonochemically-Synthesized Ultra-Stable High Internal Phase Emulsions via a Permanent Interfacial Layer. *ACS Sustainable Chem. Eng.* **2018**, *6*, 14374–14382.

(23) Patel, A. R.; Rodriguez, Y.; Lesaffer, A.; Dewettinck, K. High Internal Phase Emulsion Gels (HIPE-Gels) Prepared Using Food-Grade Components. *RSC Adv.* **2014**, *4*, 18136–18140.

(24) Chen, H. H.; Ruckenstein, E. Effect of the Nature of the Hydrophobic Oil Phase and Surfactant in the Formation of Concentrated Emulsions. *J. Colloid Interface Sci.* **1991**, *145*, 260–269.

(25) Lee, M. C.; Tan, C.; Abbaspourrad, A. Combination of Internal Structuring and External Coating in an Oleogel-Based Delivery System for Fish Oil Stabilization. *Food Chem.* **2019**, *277*, 213–221.

(26) Macierzanka, A.; Szeląg, H.; Szumała, P.; Pawłowicz, R.; Mackie, A. R.; Ridout, M. J. Effect of Crystalline Emulsifier Composition on Structural Transformations of Water-in-Oil Emulsions: Emulsification and Quiescent Conditions. *Colloids Surf., A* **2009**, *334*, 40–52.

(27) Rousseau, D. Fat crystals and emulsion stability—a review. *Food Res. Int.* **2000**, *33*, 3–14.

(28) Binks, B. P.; Rocher, A. Effects of Temperature on Water-in-Oil Emulsions Stabilised Solely by Wax Microparticles. *J. Colloid Interface Sci.* **2009**, *335*, 94–104.

(29) Lee, M. C.; Tan, C.; Abbaspourrad, A. Combination of Internal Structuring and External Coating in an Oleogel-Based Delivery System for Fish Oil Stabilization. *Food Chem.* **2019**, *277*, 213−221.
(30) Campo, V. L.; Kawano, D. F.; da Silva, D. B.; Carvalho, I. Carrageenans: Biological Properties, Chemical Modifications and Structural Analysis—A Review. *Carbohydr. Polym.* **2009**, *77*, 167−180.
(31) Chantrapornchai, W.; Clydesdale, F. M.; McClements, D. J. Influence of Flocculation on Optical Properties of Emulsions. *J. Food Sci.* **2001**, *66*, 464−469.
(32) Wrolstad, R. E. Anthocyanin Pigments-Bioactivity and Coloring Properties. *J. Food Sci.* **2006**, *69*, C419−C425.
(33) Sui, X.; Dong, X.; Zhou, W. Combined Effect of PH and High Temperature on the Stability and Antioxidant Capacity of Two Anthocyanins in Aqueous Solution. *Food Chem.* **2014**, *163*, 163−170.
(34) Tan, C.; Selig, M. J.; Lee, M. C.; Abbaspourrad, A. Polyelectrolyte Microcapsules Built on CaCO3 Scaffolds for the Integration, Encapsulation, and Controlled Release of Copigmented Anthocyanins. *Food Chem.* **2018**, *246*, 305−312.
(35) Tan, C.; Selig, M. J.; Abbaspourrad, A. Anthocyanin Stabilization by Chitosan-Chondroitin Sulfate Polyelectrolyte Complexation Integrating Catechin Co-Pigmentation. *Carbohydr. Polym.* **2018**, *181*, 124−131.
(36) Negrini, R.; Mezzenga, R. PH-Responsive Lyotropic Liquid Crystals for Controlled Drug Delivery. *Langmuir* **2011**, *27*, 5296−5303.
(37) Chang, C.-M.; Bodmeier, R. Effect of Dissolution Media and Additives on the Drug Release from Cubic Phase Delivery Systems. *J. Controlled Release* **1997**, *46*, 215−222.
(38) Tan, H.; Sun, G.; Lin, W.; Mu, C.; Ngai, T. Gelatin Particle-Stabilized High Internal Phase Emulsions as Nutraceutical Containers. *ACS Appl. Mater. Interfaces* **2014**, *6*, 13977−13984.

DOI: 10.1021/acsami.9b05089
ACS Appl. Mater. Interfaces 2019, 11, 26433−26441